Online Point Cloud Object Recognition System using Local Descriptors for Real-time Applications

Yacine Yaddaden[1,2], Sylvie Daniel[1,3] and Denis Laurendeau[1,2]
[1]*Laboratoire de Vision et Systèmes Numériques (LVSN), Université de Laval, ville de Québec, Québec, Canada*
[2]*Département de Génie Électrique et de Génie Informatique, Université de Laval, ville de Québec, Québec, Canada*
[3]*Département des Sciences Géomatiques, Université de Laval,*

Keywords: Online Machine Learning, Point Cloud Data, Unique Shape Context, Signature of Histograms of Orientation, Principal Component Analysis, *Multi-class* Support Vector Machine.

Abstract: In the context of vehicle localization based on point cloud data collected using **LiDAR** sensors, several **3D** descriptors might be employed to highlight the relevant information about the vehicle's environment. However, it is still a challenging task to assess which one is the more suitable with respect to the constraint of *real-time* processing. In this paper, we propose a system based on classical machine learning techniques and performing recognition from point cloud data after applying several *preprocessing* steps. We compare the performance of two distinct *state-of-the-art local* **3D** descriptors namely *Unique Shape Context* and *Signature of Histograms of Orientation* when combined with *online* learning algorithms. The proposed system also includes two distinct modes namely *normal* and *cluster* to deal with the point cloud data size and for which performances are evaluated. In order to measure the performance of the proposed system, we used a benchmark **RGB-D** object dataset from which we randomly selected three *stratified* subsets. The obtained results are promising and suggesting further experimentation involving real data collected from **LiDAR** sensors on vehicles.

SCITEPRESS SCIENCE AND TECHNOLOGY PUBLICATIONS

1 INTRODUCTION

During the last decades, we have witnessed the emergence of new acquisition devices and *sensors* which allow to capture more reliable and relevant information. Indeed, new camera models (such as the *Microsoft Kinect*) and *wide range sensors* are employed to capture *depth* information. Moreover, these sensors are becoming more affordable which leads to create new fields of application. One of the most interesting use of this kind of sensors remains *autonomous vehicle* or *self-driving car* (Lee et al., 2016). Several systems have been proposed aiming to exploit the potential of *depth* information in order to avoid obstacles or for localization (Wolcott and Eustice, 2014).

The main aim of this work lies in developing an efficient recognition system from point cloud data that will be used in the context of *driving assistance* and, more precisely, for localization in *real-time*. In this paper, we present a comparison in terms of performance of the proposed system when using different techniques in the processing blocks. Indeed, we compare two distinct *local* **3D** descriptors namely **USC** and **SHOT** (including the color version **SHOT**-*rgb*) for data representation. We also compare two operating modes, namely *normal* and *cluster*, in order to deal with variable size of the point cloud. However, the most important improvement in comparison to traditional systems lies in the use of *incremental* or *online* versions of the learning algorithms. They allow to tackle the memory issue caused by processing huge amounts of data. In order to evaluate the performance of the proposed system, we use a common and publicly available benchmark **RGB-D** dataset (Lai et al., 2011).

The remainder of the paper is structured as follows. In section 2, we present basic notions about recognition systems from point cloud data. Section 3 details each component of the proposed system. Sections 4 and 5 are dedicated to the description of the experimental protocol for system evaluation with several metrics and the discussion of the results. Finally,

Yaddaden, Y., Daniel, S. and Laurendeau, D.
Online Point Cloud Object Recognition System using Local Descriptors for Real-time Applications.
DOI: 10.5220/0010198703010308
In *Proceedings of the 16th International Joint Conference on Computer Vision, Imaging and Computer Graphics Theory and Applications (VISIGRAPP 2021) - Volume 5: VISAPP*, pages 301-308
ISBN: 978-989-758-488-6
Copyright © 2021 by SCITEPRESS – Science and Technology Publications, Lda. All rights reserved

in section 6 concluding remarks and further works are presented.

2 BACKGROUND

2.1 Fundamentals

Object recognition systems from point cloud data consist of the same building blocks as those of common pattern recognition system. Indeed, they include an *input* which is fed by raw point cloud data and an *output* which represents the label of the recognized object. Between them, there are several processing blocks, some of which are mandatory and other optional. The *preprocessing* block aims to prepare and clean up the input point cloud data before the *feature extraction* step. This building block is critical since it aims to generate an efficient and robust representation using either *handcrafted* descriptors (Guo et al., 2016) or new *deep learning* techniques (Zaki et al., 2016) and (Schwarz et al., 2015). In order to reduce the size of the generated representation to optimize the computation time, *dimension reduction* is employed to highlight discriminant information while getting rid of the redundant one. Finally, the *classification* block exploits a *supervised* machine learning technique to perform recognition (Maturana and Scherer, 2015).

Working with point cloud data and *depth* information is not new. In fact, several **3D** descriptors have already been proposed in order to provide a reliable representation from raw data. Moreover, numerous works have been conducted in order to provide an accurate comparison in terms of performance of *state-of-the-art* and most common **3D** descriptors (Guo et al., 2016), (Hana et al., 2018) and (Carvalho and von Wangenheim, 2019). We distinguish three different categories of descriptors: 1) *local* descriptors which encode the local geometric information at each point based on its neighbors, 2) *global* features (do Monte Lima and Teichrieb, 2016) that highlight the geometric information of the whole **3D** point cloud, 3) *hybrid* descriptors (Alhamzi et al., 2015) which combine and group the essential information provided by both previous representations in the sake of performance improvement. Each one has its strengths and limitations. Indeed, *local* descriptors are more robust and less sensitive to partial occlusion, but remain computationally inefficient in comparison to *global* ones. The computational inefficiency of *local* descriptors lies in the huge size of the extracted representation. However, it is possible to get rid of this flaw by reducing the size of the generated representation by applying *dimension reduction*.

It is important to highlight the fact that depending on the field of application, the point cloud size might vary. Indeed, when using point cloud data collected with **LiDAR** sensors in the context of localization, the amount of data is too large to be processed in one shot. Usually, in order to deal with this type of situation, the point cloud is *partitioned* using dedicated techniques, then each segment is processed individually. However, in the case of small object recognition, the partitioning step is not required.

As mentioned above, several descriptors can be used in order to generate a relevant representation from point cloud data and choosing the most adequate one is tough since it depends on the context. In our case, details are important and contribute to improve the discrimination capability of the developed system when performing localization. Thus, the choice of *local* **3D** descriptors seems adequate. The *hybrid* ones might also do the job, but in the context of *real-time* application, reducing the amount of computation is mandatory and combining two descriptors does not help. Among all the existing *local* **3D** descriptors, we chose **USC** for its capability to decrease memory requirement while improving accuracy (Guo et al., 2014). As for our primary choice, we chose **SHOT** and its *color* version **SHOT**-*rgb* since it is highly descriptive, computationally efficient and robust to noise (Guo et al., 2014), (Alexandre, 2012) and (Hana et al., 2018).

USC stands for *Unique Shape Context* and consists in a *local* **3D** descriptor proposed by (Tombari et al., 2010). **USC** is an improvement and optimization of the **3DSC** (Frome et al., 2004) aiming to reduce the computational load. In order to generate this representation, the first step consists in constructing a **LRF** *(Local Reference Frame)* before aligning the neighboring points to ensure invariance to translations and rotations. As shown in Figure 1a, the neighborhood of the keypoint from which is extracted the descriptor is divided into several *bins*. The final *histogram* is computed by accumulating the weighted sum of the points in each bin.

SHOT or *Signature of Histograms of OrienTation* is also a *local* **3D** descriptor introduced by (Salti et al., 2014). It is one of the most effective **3D** features in terms of descriptiveness and computational efficiency (Hana et al., 2018). Just like the **USC** descriptor, the first step consists in the construction of a **LRF** and aligning the neighboring points. As shown in Figure 1b, the *sphere* around the keypoint is divided into several volumes along the *azimuth*, *radial* and *elevation axes*. Then, for each volume, a local histogram is

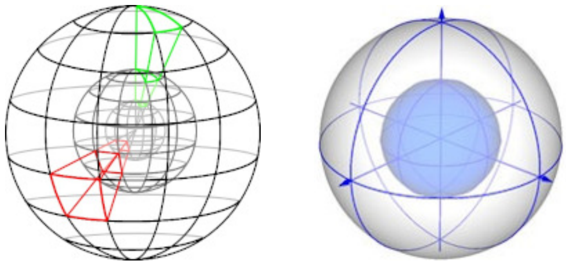

(a) **3DSC** descriptor. (b) **SHOT** descriptor.

Figure 1: The *local* **3D** descriptor representations.

computed by counting the points into *bins* according to the angles between the normals at the neighboring points inside the volume and the normal at the keypoint. The last step consists in concatenating all the local histograms.

One of the common issues when working with point cloud data lies in the huge number of points to process. In order to deal with this situation, *keypoints selection* has to be included in the system's building blocks in order to reduce the size of the input data and at the same time improving computer efficiency. Basically, it consists in selecting a certain amount of points from the initial point cloud using a specific technique. Then, instead of generating the representation from a large point cloud, the operation is performed on a smaller one. Several techniques exist and might be employed, (Filipe and Alexandre, 2014) presented an accurate comparison in terms of performance. Among the different existing techniques we find: **Harris3D**, **SUSAN**, **SIFT3D** and **ISS3D**, the best performance being achieved by the two latter techniques. However, the presented list is not exhaustive and several other techniques might be used.

2.2 Related Works

As discussed previously, there are several building blocks for object recognition systems applied to point cloud data. Besides, we distinguish two categories of *pipelines*. The *traditional* one is based on *handcrafted* representation and classic learning techniques for recognition. (Chen et al., 2018) have employed several *local* **3D** descriptors, among which figure the **USC** and **SHOT**, in order to perform construction object recognition. Moreover, they used *matching learning* techniques for recognition. (Cop et al., 2018) proposed a new system called **DELIGHT** that allows a robot to estimate its position based on **LiDAR** data and using the **SHOT** descriptor. Similarly, (Guo et al., 2019) proposed a localization system in the context of mobile robotics using a new *local* **3D** descriptor **ISHOT** (*Intensity* **SHOT**). It yields the best performances when compared with other **3D** descriptors. (Garstka. and Peters., 2016) have compared the performance of several *local* **3D** descriptors for object recognition using the same *pipeline* described above. In the context of object manipulation by robots, (Costanzo. et al., 2018) proposed a *hybrid* and *real-time* object recognition system.

The second category of *pipeline* consists in using *deep learning* techniques which offer better recognition rates but requires high performance computational hardware. (Zaki et al., 2016) and (Schwarz et al., 2015) have introduced systems based on **CNN** *(Convolutional Neural Network*) architectures. (Guo et al., 2020) also presented an interesting comparison of *deep learning* based systems in the context of recognition from point cloud data. Among them are the following architectures: PointNet++ (Qi et al., 2017), VoxNet (Maturana and Scherer, 2015), etc.

To our knowledge, most of the existing methods which allow processing point cloud data in the context of object recognition or vehicle localization, have as main focus the improvement of the accuracy. In our case, we are more interested in enabling and improving the *real-time* capability of the proposed system.

3 PROPOSED SYSTEM

In this paper, we introduce a system allowing automatic recognition of common everyday objects from *point cloud data*. After validation, it is intended to be used for assisting bus drivers by performing accurate localization even under adverse climatic conditions. As shown in Figure 2, the system includes several processing blocks which we describe in this section.

3.1 Preprocessing

The number of points per point cloud varies and since we are working with *local* **3D** descriptors, the size of the generated representation varies as well. Moreover, the some next processing blocks, namely *dimension reduction* and *classification* require a constant feature vector size. In order to deal with this issue, we propose two different operating modes called *normal* and *cluster*.

In the *normal* mode, the system applies *downsampling* which aims to reduce the size of the point cloud data. Basically, the employed technique creates a **3D** *voxel grid*. Then, in each *voxel*, all the points present will be approximated with their *centroid*. In the context of the object dataset that we are using for evaluation, we set *empirically* the parameter that sets the

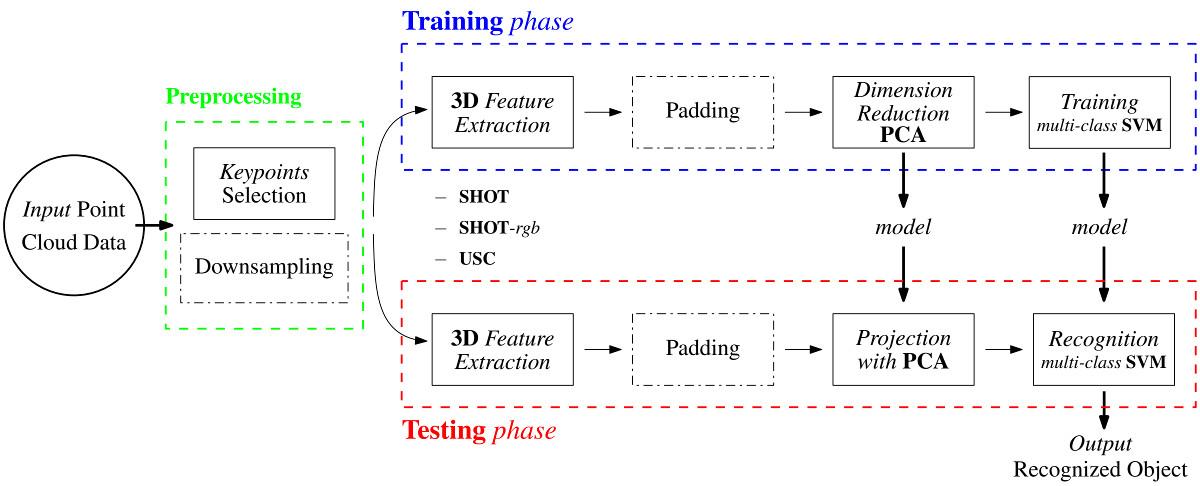

Figure 2: Overview of the proposed *point cloud recognition* system.

size of each *voxel* to $d = 0.5$ *cm*. This step is important since it reduces the computing time by getting rid of redundant data. Even with such an approach, the size of the input vectors remains variable. To compensate for this, we apply a simple *zero padding* operation after performing the *feature extraction* step.

As shown in Figure 3, the *cluster* mode applies the k-means algorithm to the point cloud data (in *blue*). It consists in an *unsupervised* machine learning technique that identifies similar instances or *points* and assigns them to a *cluster* (in *red*) using a specific metric (*euclidean distance*). After applying k-means, the closest point (*black circles*) to the *centroid* (*green squares*) is selected for each cluster. In this case, *downsampling* is not applied for the sake of keeping all the details. Thus, for each one of the selected *keypoints*, a *local* descriptor will be computed in the next step based on all the neighboring points within the defined radius. Similarly as the *normal* mode, the number of clusters k involved in the k-means algorithm needs to be set empirically ($k = 50$ for the object dataset used for evaluation).

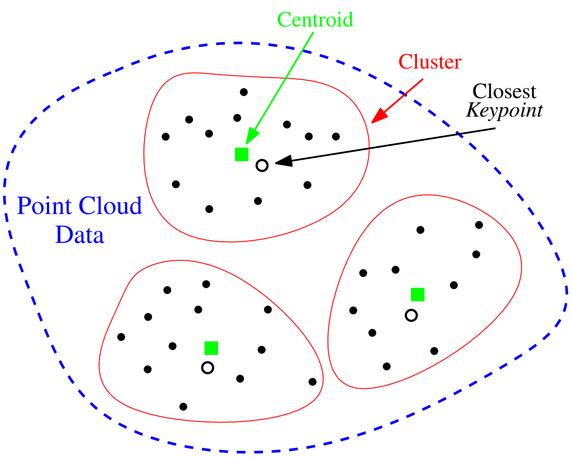

Figure 3: Overview of the *keypoints selection* process.

3.2 Feature Extraction

In order to optimize the performance of the system in terms of recognition, an efficient representation of the input is required. The proposed system allows the extraction of two distinct *local* **3D** descriptors namely **USC** (Tombari et al., 2010) and **SHOT** (Salti et al., 2014) (including the color version **SHOT**-*rgb*). Since the generation of both representations implies that the neighbors around the concerned point be taken into account, we need to set *empirically* the *search radius* parameter (in our case $r = 1.0$ *cm*).

Both descriptors generate an *histogram* for each point and the size of these descriptors, related to the histogram number of bins, is different. More precisely, here is the size of the related histograms: $|V_{USC}| = 1980$, $|V_{SHOT}| = 352$ and $|V_{SHOT-rgb}| = 1344$ *bins*. The final feature vector consists of a *concatenation* of all histograms. However, this last operation varies depending on the selected mode. In the case of *normal* mode, the concatenation is performed on all the histograms generated from all the points after *downsampling*. Then, since the number of points is not the same, a *zero padding* operation is applied. For the *cluster* mode, the number of *keypoints* is always the same as initially defined. Therefore, the *concatenation* is performed only on the histograms generated from these *keypoints*.

3.3 Dimension Reduction

The size of the generated representation using the chosen **3D** descriptors namely **USC** and **SHOT** (including the color version **SHOT**-*rgb*) is huge considering the number of keypoints and the size of histograms. Therefore, we need to reduce its size to ease and optimize the recognition performance. Even if several *dimension reduction* techniques exist, the most commonly used is the **PCA** *(Principal Components Analysis)* (Jolliffe and Cadima, 2016). It is defined as an *unsupervised*, *non-parametrical* statistical technique used in machine learning aiming to identify the *hyperplane* such that the variance of the data when projected onto this plane is changed as little as possible. The generated axes or *principal components* are *orthogonal*. The reduced feature vector which consists in a certain number of *principal components* feeds the *classification* block.

Taking into account the number of samples and the size of previously generated representations, applying the standard version of the **PCA** might lead to memory issues. Therefore, we propose to use the *incremental* or *online* version which allows to apply **PCA** in an *iterative* way by taking as input small *batches* of samples (from the dataset).

3.4 Classification

In order to perform recognition based on the reduced representation, we use a *classification* technique. It consists in a *supervised* machine learning technique which requires a *learning* phase using labeled data. Even if several techniques might be used, we adopt the *multi-class* and *linear* **SVM** *(Support Vector Machine)* since it yields relatively good performance. It has been proposed by (Cortes and Vapnik, 1995) as a *binary* classifier aiming to find a *hyperplane* to optimally separate two distinct classes. It might be defined by $y_i = sign(\langle \mathbf{w}, x_i \rangle + b)$ where the *maximum-margin hyperplane* is represented by $(\mathbf{w}, b)$, the feature vectors by $x_i \in \mathbb{R}^d$ and labels by $y_i \in \{\pm 1\}$. In order to distinguish between several objects, we adopt the *One-Against-All* architecture which consists of several *linear binary*-**SVM** classifiers.

Similarly to the **PCA** and in order to deal with huge amount of *samples*, we adopt the *online* version of the *multi-class* **SVM**.

4 EVALUATION

In order to evaluate the proposed system in both modes namely *normal* and *cluster*, we used the benchmark and publicly available **RGB-D**[1] dataset (Lai et al., 2011) (see Figure 4). It consists of 300 common

Figure 4: Overview of the **RGB-D** dataset (Lee et al., 2016).

everyday objects organized in 51 distinct categories. The samples are collected using a *Kinect*-style camera enabling the emphasis of *depth* information. The type of sensors employed to collect the used dataset is not the same as the one we are targeting and which consists in **LiDAR** sensors. However, the data format is the same since the **LiDAR** sensors also collect point cloud data. The main differences when using these two types of sensors lies the covered range and density. Moreover, the main aim of this work consists in validating the systems and defining the most suitable configuration in terms of *mode*, descriptor and algorithm version. Therefore, in order to speed up the evaluation, we selected three different *stratified* subsets namely: *first subset* (greens, pliers, food_jar, hand_towel and toothpaste), *second subset* (binder, sponge, camera, kleenex and lemon) and *third subset* (water_bottle, scissors, banana, flashlight and bowl). Each one contains 250 different samples. The choice of the different objects and samples for each subset is made in a *random manner*.

As for the evaluation metrics, we employed several ones. Usually, the most important one is related to the recognition rate. Thus, we compute the *accuracy* which represents the number of correct predictions divided by the total number of samples. Moreover, since the proposed system performs *multi-class* classification, the recognition rate for each object is also provided. The accuracy might be biased if the system performs better with certain classes than for the others. Therefore, by computing the *average* of all the objects recognition rate, we provide more precision about the system performances. Furthermore, since we are targeting *real-time* application, we also measured the elapsed time when performing learning and evaluation with different system configurations.

As for the evaluation protocol, we adopted the *k-fold cross-validation splitting strategy*. We set the number of folds to $k = 5$ and therefore, each one of the three sets of data (namely *first subset*, *second subset* and *third subset*) is divided into *five* subsets. During each iteration, *four* subsets are used for training and

[1] https://rgbd-dataset.cs.washington.edu/dataset.html

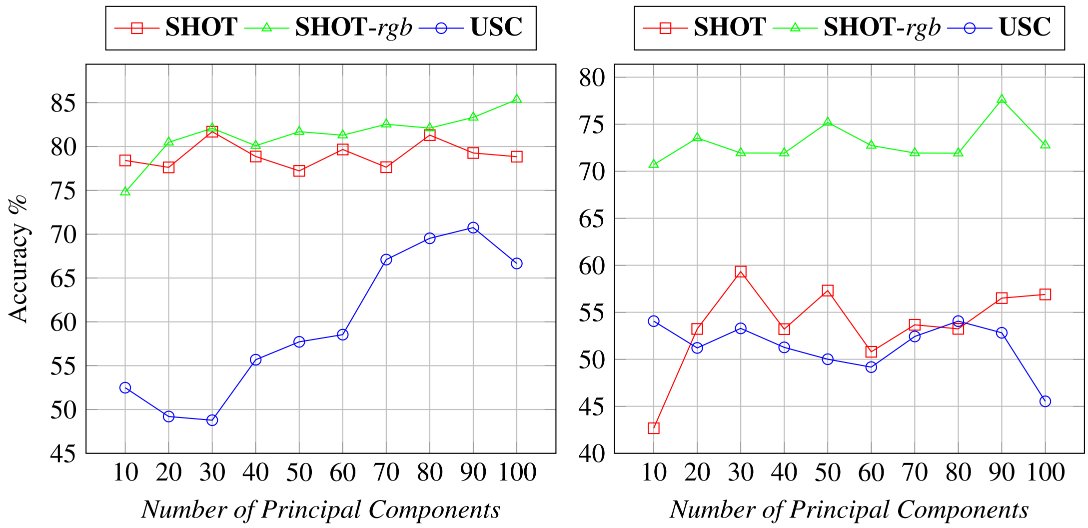

(a) Using *normal* mode.

(b) Using *cluster* mode.

Figure 6: Accuracy per number of principal components.

the last one for evaluation. The final accuracy of each set of data is computed by averaging the obtained accuracy at each iteration.

5 RESULTS AND DISCUSSION

In this section, we present and discuss the results obtained after performing several evaluations. Each one focusing on a specific metric.

Figure 5 displays system performance in terms of accuracy when using the two *local* **3D** descriptors in both working modes (*normal* and *cluster*). We notice that the highest accuracy is achieved by the **SHOT**-*rgb* descriptor in both modes. Indeed, it allows to reach 87.55% and 71.54% in *normal* and *cluster* mode, respectively. The reason might be explained by the additional color information provided by **SHOT**-*rgb*. As for the **USC** descriptor, it yields the lowest accuracy.

In Figures 6a and 6b is shown the variation of accuracy for the two *local* **3D** descriptors in both working modes (*normal* and *cluster*) regarding the number of *principal components*. Similarly to Figure 5, the best performance is achieved by the **SHOT**-*rgb* descriptor in *normal* mode. We also notice how the **PCA** contributes to compress the feature vectors and highlights the relevant and discriminant information. Thus, we are able to obtain a relatively good accuracy using only a few attributes or *principal components*. From both Figures 6a and 6b, we notice that there is not a constant and regular increase when adding more principal components. It might be explained by the

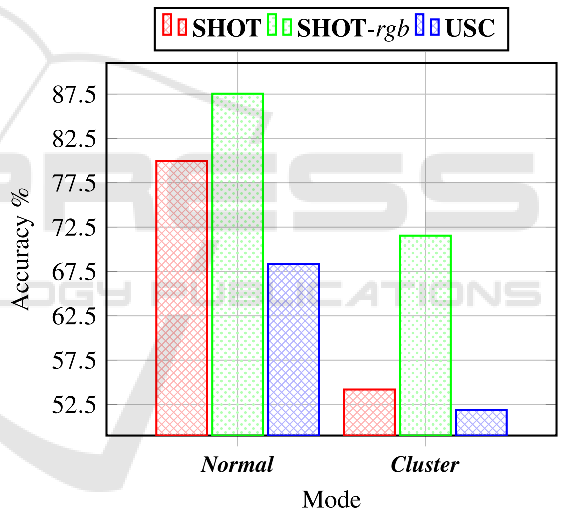

Figure 5: Comparison of both modes (*normal* & *cluster*).

fact that adding more attributes or variables does not necessarily improve the accuracy since some of them introduces noise to the classifier.

Table 1 provides details on the recognition rates for each *subset* and *objects*. We notice that the **SHOT**-*rgb* descriptor achieves relatively high accuracy with 92.17% in the *second subset*. As for the recognition rate for each object, we notice that for certain objects (pliers, lemon, hand_towel), the highest accuracy of 100.00% is achieved. Based on the obtained results in the different *subsets*, there is an average difference of $\approx 8.00\%$ between the *normal* and *cluster* mode.

In Table 2 are shown the results relevant to the *computational efficiency* of the proposed system. One

Table 1: Accuracy comparison between the three subsets & both modes.

Mode	***Descriptors***	***Objects recognition rates (%)***					***Average (%)***	***Accuracy (%)***
First subset		greens	pliers	food_jar	hand_towel	toothpaste	-	-
Normal	**SHOT**	95.83	100.00	64.81	95.56	55.56	82.35	82.52
Cluster		47.92	98.15	50.00	51.11	44.44	58.32	59.33
Normal	**SHOT**-*rgb*	95.83	100.00	75.93	100.00	62.22	86.80	**87.00**
Cluster		85.42	98.15	44.44	100.00	62.22	78.05	**77.62**
Normal	**USC**	81.25	100.00	55.56	91.11	40.00	73.58	73.98
Cluster		31.25	92.59	81.48	46.67	6.67	51.73	54.06
Second subset		binder	sponge	camera	kleenex	lemon	-	-
Normal	**SHOT**	74.07	75.00	72.22	86.67	98.15	81.22	81.44
Cluster		42.59	27.78	53.70	37.78	88.89	50.15	52.25
Normal	**SHOT**-*rgb*	74.07	94.44	94.44	100.00	100.00	92.59	**92.17**
Cluster		72.22	33.33	70.37	68.89	92.59	67.48	**69.95**
Normal	**USC**	74.07	55.56	31.48	88.89	100.00	70.00	70.37
Cluster		59.26	0.00	64.81	15.56	75.93	43.11	47.30
Third subset		water_bottle	scissors	banana	flashlight	bowl	-	-
Normal	**SHOT**	77.78	81.25	50.00	68.89	98.15	75.21	75.89
Cluster		50.00	81.25	31.25	28.89	61.11	50.50	51.00
Normal	**SHOT**-*rgb*	83.33	83.33	68.75	91.11	90.74	83.45	**83.49**
Cluster		77.78	87.50	66.67	31.11	68.52	66.32	**67.06**
Normal	**USC**	38.89	52.08	41.67	68.89	100.00	60.31	60.65
Cluster		57.41	91.67	68.75	17.78	35.19	54.16	54.22

of the main differences between the *normal* and *cluster* modes lies in the feature vectors size. Indeed, the latter mode is less complex since the descriptor vector size is relatively smaller than the former one. The smallest vector size is associated with **SHOT**. Indeed, it is 3.8× and 5.5× smaller than **SHOT**-*rgb* and **USC**, respectively. The other criteria that is considered is the computing time. The **SHOT** descriptor takes the less time in comparison to the others. As for the *online* version (see the second line for each descriptor in Table 2), even if it deals with the memory issue, it slightly reduces the accuracy and increases the computing time.

Table 2: *Computing time* and *vector size* comparison.

Mode	***Descriptors***	***Time (ms)***	***Vector Size***	***Accuracy (%)***
Normal	**SHOT**	38	574112	**82.53**
		65		72.80
	SHOT-*rgb*	90	2192064	**87.00**
		189		78.47
	USC	113	3196760	**73.98**
		286		65.09
Cluster	**SHOT**	238	17600	**59.33**
		241		43.12
	SHOT-*rgb*	257	67200	**77.62**
		264		71.54
	USC	657	98000	**54.06**
		666		42.26

Taking into account all the evaluation criteria, we suggest that the most suitable system needs to combine the **SHOT** descriptor and the *online* versions of both **PCA** and *multi-class* **SVM**.

6 CONCLUDING REMARKS

In this paper, we introduce an object recognition system from point cloud data. We compare two *local* **3D** descriptors namely **USC** and **SHOT** (including the color version **SHOT**-*rgb*) and show through experiments that the latter performs better. We also propose two different modes namely *normal* and *cluster*. The former one performs better in terms of accuracy, but the second one allows to reduce considerably the size of the input point cloud. We overcome the memory issue when working with huge amount of data by using *incremental* versions of **PCA** and *multi-class* **SVM**. As further works, we are planning on using the proposed system on **LiDAR** data in the context of vehicle localization. We also intend to optimize the proposed system in order to increase its performances.

ACKNOWLEDGEMENTS

This work was supported by NSERC Collaborative Research and Development grant **CRDPJ 511843 – 17**. We also acknowledge the providers of the used benchmark **RGB-D** Object Dataset (Lai et al., 2011).

REFERENCES

Alexandre, L. A. (2012). 3d descriptors for object and category recognition: a comparative evaluation. In *Workshop on Color-Depth Camera Fusion in Robotics at the IEEE/RSJ International Conference on Intelligent Robots and Systems (IROS), Vilamoura, Portugal*, volume 1, page 7.

Alhamzi, K., Elmogy, M., and Barakat, S. (2015). 3d object recognition based on local and global features using point cloud library. *International Journal of Advancements in Computing Technology*, 7(3):43.

Carvalho, L. and von Wangenheim, A. (2019). 3d object recognition and classification: a systematic literature review. *Pattern Analysis and Applications*, 22(4):1243–1292.

Chen, J., Fang, Y., and Cho, Y. K. (2018). Performance evaluation of 3d descriptors for object recognition in construction applications. *Automation in Construction*, 86:44–52.

Cop, K. P., Borges, P. V., and Dubé, R. (2018). Delight: An efficient descriptor for global localisation using lidar intensities. In *2018 IEEE International Conference on Robotics and Automation (ICRA)*, pages 3653–3660. IEEE.

Cortes, C. and Vapnik, V. (1995). Support-vector networks. *Machine learning*, 20(3):273–297.

Costanzo., M., Maria., G. D., Lettera., G., Natale., C., and Pirozzi., S. (2018). Flexible motion planning for object manipulation in cluttered scenes. In *Proceedings of the 15th International Conference on Informatics in Control, Automation and Robotics - Volume 1: ICINCO,*, pages 110–121. INSTICC, SciTePress.

do Monte Lima, J. P. S. and Teichrieb, V. (2016). An efficient global point cloud descriptor for object recognition and pose estimation. In *2016 29th SIBGRAPI Conference on Graphics, Patterns and Images (SIBGRAPI)*, pages 56–63. IEEE.

Filipe, S. and Alexandre, L. A. (2014). A comparative evaluation of 3d keypoint detectors in a rgb-d object dataset. In *2014 International Conference on Computer Vision Theory and Applications (VISAPP)*, volume 1, pages 476–483. IEEE.

Frome, A., Huber, D., Kolluri, R., Bülow, T., and Malik, J. (2004). Recognizing objects in range data using regional point descriptors. In *European conference on computer vision*, pages 224–237. Springer.

Garstka., J. and Peters., G. (2016). Evaluation of local 3-d point cloud descriptors in terms of suitability for object classification. In *Proceedings of the 13th International Conference on Informatics in Control, Automation and Robotics - Volume 2: ICINCO,*, pages 540–547. INSTICC, SciTePress.

Guo, J., Borges, P. V., Park, C., and Gawel, A. (2019). Local descriptor for robust place recognition using lidar intensity. *IEEE Robotics and Automation Letters*, 4(2):1470–1477.

Guo, Y., Bennamoun, M., Sohel, F., Lu, M., and Wan, J. (2014). 3d object recognition in cluttered scenes with local surface features: a survey. *IEEE Transactions on Pattern Analysis and Machine Intelligence*, 36(11):2270–2287.

Guo, Y., Bennamoun, M., Sohel, F., Lu, M., Wan, J., and Kwok, N. M. (2016). A comprehensive performance evaluation of 3d local feature descriptors. *International Journal of Computer Vision*, 116(1):66–89.

Guo, Y., Wang, H., Hu, Q., Liu, H., Liu, L., and Bennamoun, M. (2020). Deep learning for 3d point clouds: A survey. *IEEE Transactions on Pattern Analysis and Machine Intelligence*.

Hana, X.-F., Jin, J. S., Xie, J., Wang, M.-J., and Jiang, W. (2018). A comprehensive review of 3d point cloud descriptors. *arXiv preprint arXiv:1802.02297*.

Jolliffe, I. T. and Cadima, J. (2016). Principal component analysis: a review and recent developments. *Philosophical Transactions of the Royal Society A: Mathematical, Physical and Engineering Sciences*, 374(2065):20150202.

Lai, K., Bo, L., Ren, X., and Fox, D. (2011). A large-scale hierarchical multi-view rgb-d object dataset. In *2011 IEEE international conference on robotics and automation*, pages 1817–1824. IEEE.

Lee, U., Jung, J., Shin, S., Jeong, Y., Park, K., Shim, D. H., and Kweon, I.-s. (2016). Eurecar turbo: A self-driving car that can handle adverse weather conditions. In *2016 IEEE/RSJ International Conference on Intelligent Robots and Systems (IROS)*, pages 2301–2306. IEEE.

Maturana, D. and Scherer, S. (2015). Voxnet: A 3d convolutional neural network for real-time object recognition. In *2015 IEEE/RSJ International Conference on Intelligent Robots and Systems (IROS)*, pages 922–928. IEEE.

Qi, C. R., Yi, L., Su, H., and Guibas, L. J. (2017). Pointnet++: Deep hierarchical feature learning on point sets in a metric space. In Guyon, I., Luxburg, U. V., Bengio, S., Wallach, H., Fergus, R., Vishwanathan, S., and Garnett, R., editors, *Advances in Neural Information Processing Systems*, volume 30, pages 5099–5108. Curran Associates, Inc.

Salti, S., Tombari, F., and Di Stefano, L. (2014). Shot: Unique signatures of histograms for surface and texture description. *Computer Vision and Image Understanding*, 125:251–264.

Schwarz, M., Schulz, H., and Behnke, S. (2015). Rgb-d object recognition and pose estimation based on pre-trained convolutional neural network features. In *2015 IEEE international conference on robotics and automation (ICRA)*, pages 1329–1335. IEEE.

Tombari, F., Salti, S., and Di Stefano, L. (2010). Unique shape context for 3d data description. In *Proceedings of the ACM workshop on 3D object retrieval*, pages 57–62.

Wolcott, R. W. and Eustice, R. M. (2014). Visual localization within lidar maps for automated urban driving. In *2014 IEEE/RSJ International Conference on Intelligent Robots and Systems*, pages 176–183. IEEE.

Zaki, H. F., Shafait, F., and Mian, A. (2016). Convolutional hypercube pyramid for accurate rgb-d object category and instance recognition. In *2016 IEEE International Conference on Robotics and Automation (ICRA)*, pages 1685–1692. IEEE.